

Josephson Vortices in High T_c Superconductors

Kazuto Hirata

National Institute for Materials Science, Tsukuba
Japan

1. Introduction

When a magnetic field is applied to the type-II superconductors in a superconducting state, the magnetic field penetrates into the superconductors above the first critical field H_{c1} , and is quantized in a unit of ϕ_0 ($=h/2e=2.07 \times 10^{-7}$ gauss-cm²). This is a general view of magnetic flux (vortex) in the type-II superconductors as schematically drawn in Fig.1 (a). The wave function of superconductivity Φ extends to the coherence length ξ , and the applied magnetic field H is screened by the supercurrent in a range of the penetration depth of λ from the center of vortex core. In this case, vortex has a core of normal state. In a lower magnetic field, vortices behave as isolated vortices. When the magnetic field becomes higher, interaction between/among vortices, vortices form „Abrikosov“ vortex lattice in triangular or square distribution, which has been observed by scanning tunneling microscope (Hess et al. 1994) and small angle neutron scattering (Yethiraj et al, 1993) mainly in mettalic and intermetallic superconductors.

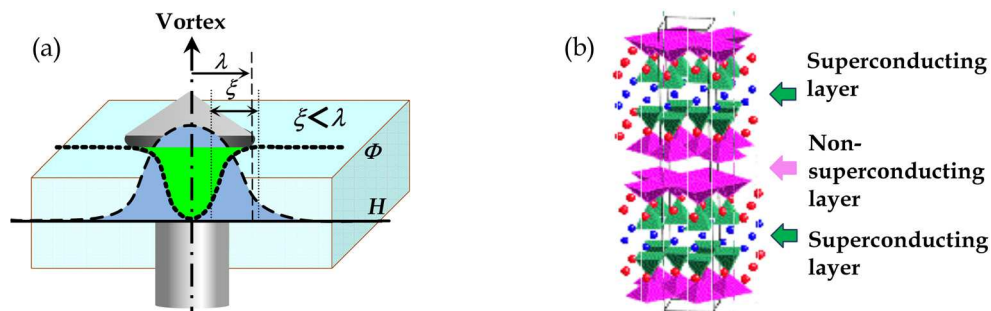


Fig. 1. Schematic drawing of a magnetic flux (vortex) in type-II superconductor (a) and the crystal structure of $\text{Bi}_2\text{Sr}_2\text{CaCu}_2\text{O}_{8+\delta}$ (b).

High-temperature superconductors (HTSCs) also belong to the type-II superconductors. However, vortex state is quite different from that in conventional superconductors. This has mainly its origin in the layered crystal structures in atomic scale. The crystal structure of HTSCs is consisted of the Cu-O superconducting layers and the nonsuperconducting ones iteratively as shown in Fig.1 (b). It causes a weak Josephson coupling between the Cu-O superconducting layers through the insulating layers in superconducting state. This leads intrinsically to the nanoscale Josephson junctions (JJs) in crystalline unit cells, and also induces a strong anisotropy of physical properties in HTSCs.

When the magnetic field is applied perpendicular to the superconducting layers of HTSCs, vortices in the superconducting layer distribute in a regular two-dimensional (2D) lattice of triangular or square as in the case of conventional superconductors. However, along the perpendicular direction to the layers, flux line is connected weakly to each other with pancake vortex in each layer. Vortices of HTSCs in the perpendicular field are called as pancake vortices (PVs). In the parallel field, based on the layered structure of HTSCs, namely, intrinsic Josephson junctions (IJJs) (Kleiner et al., 1992; Rapp et al. 1996), vortices shown in Fig.2 (a) behave as those in the Josephson junctions artificially made of superconductor/insulator/superconductor structure. In the JJs, Josephson vortex (JV) is formed in a characteristic state of vortex without normal state core (Bulaevskii & Clem 1991; Koshelev 2000). JV is contracted along the direction perpendicular to the layers and extends to the direction parallel to the layers, depending on the anisotropy. Details are described in section 3.1.

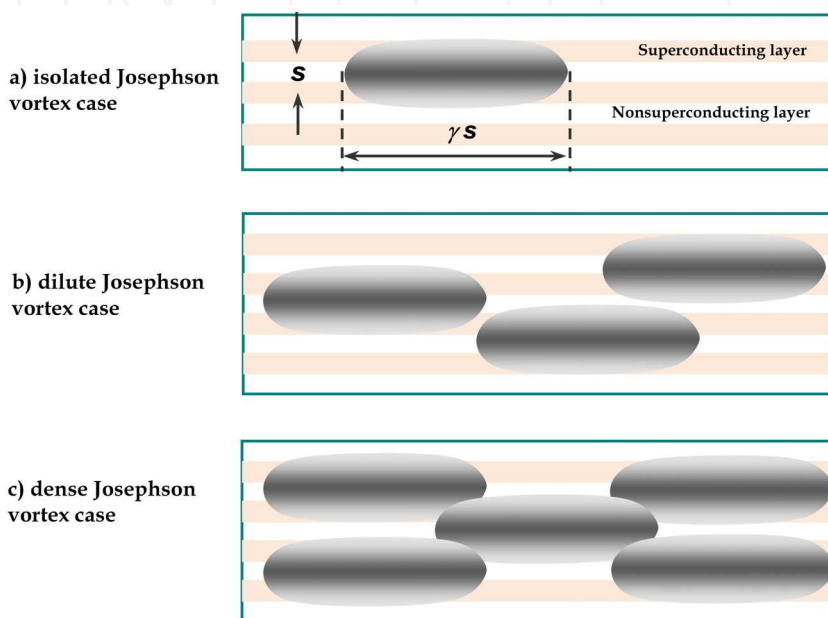


Fig. 2. Schematic drawing of distribution of Josephson vortices with a) isolated, b) dilute, and c) dense case.

Even in the perpendicular field to the superconducting layers, HTSCs show distinguished features of PVs in the vortex state. The first-order melting transition of PV-lattice (Zeldov et al. 1995), Bragg glass phase and vortex glass phase (Blatter et al. 1994) have been made clear experimentally and theoretically. In the parallel fields to the layers, magnetic field penetrates as JVs in a superconducting state of HTSCs. Theoretical studies have been made extensively from just after the discovery of HTSCs. Thermally-activated disordered vortex state, Kosterlitz-Thouless (K-T) transition in the smectic vortex state (Blatter et al. 1994; Balents & Nelson 1995), new vortex phases and a change of a tri-critical point in the dimension of the melting transition (Hu & Tachiki 2000) and the K-T type phase and the melting of 2D quasi-lattice have been predicted theoretically (Ivlev et al. 1990; Hu &

Tachiki 2004). However, JV system has not been understood well experimentally. The melting transition of the JV system (Kwok et al. 1994), the oscillatory melting temperature (Gordeev et al. 2000), and the vortex smectic phase have been found only in $\text{YBa}_2\text{Cu}_3\text{O}_{7-\delta}$ (YBCO). In strongly anisotropic HTSCs such as $\text{Bi}_2\text{Sr}_2\text{CaCu}_2\text{O}_{8+\delta}$ (Bi-2212), few experimental results have been reported on the magnetic phases of the JV system (Fuhrer et al. 1997; Mirkovic et al. 2001).

Most of the difficulties to study on JV system in experiments are considered due to a little change of physical parameters at the phase boundary. Shear modulus of JVs between the layers is very little and it is considered that a change in free energy is so small at the boundary to be observed by the experiments (Shilling et al. 1997). Recently we have found a new method to study the magnetic phases of JV system by using the periodic oscillations in flow resistance of JVs (Ooi et al. 2002), from which we can deduce the configurations of JVs. This phenomenon is caused by the intrinsic boundary effect of the sample, related to the configurations of JVs (Ooi et al. 2002; Koshelev 2002; Machida 2003). The magnetic phase, in which the periodic oscillations are observed, has been confirmed as a three-dimensional (3D) ordered vortex state. The periodic oscillations are observed independent to temperature and magnetic field, which is a universal nature of JV flow-resistance. Then, it is useful for determining an absolute magnetic field. In this chapter, experimental methods for observing the periodic oscillations and for fabricating the sample for the measurements are described in section 2, general view of vortex flow in section 3, magnetic phases in section 4, application of the periodic oscillations in section 5, and finally conclusion in section 6.

2. Experimental method

Single crystals of Bi-2212 were grown with a travelling solvent floating zone method (Mochiku et al., 1997). The crystals have been cut and cleaved into the platelets with a thickness of about $20\mu\text{m}$ and an area of about $5\text{mm} \times 3\text{mm}$. Samples for the focused ion beam (FIB) structuring were obtained by dicing the platelets into small pieces of a bar-shape with an area of about $50\mu\text{m} \times 3\text{mm}$. The superconducting transition temperature (T_c) of the samples is about 85K. After four electrodes have been put on the bar by silver paste, IJJs have been fabricated at the center of the bar by using FIB as shown in Fig.3 (a). Detailed fabrication is described elsewhere (Kim et al. 1999). In the inset of Fig. 3 (a) and Fig.3 (b), a schematic drawing IJJ of the in-line symmetric type is shown used for four-probe measurements in the applied field H with ac (13 Hz:LR-700 AC resistance bridge) and dc current (Keithley 2400). Since the resistance of the IJJ part is 3 orders larger than that of the other part, we can measure the flow resistance of the IJJ part along the c -axis of the single crystal mainly as shown in Fig.3 (b).

The samples have been aligned to the parallel field by measuring the flow resistance at constant field and current as a function of relative angle. When the field is close to parallel to the layers, JVs are in a lock-in state (Hechtfisher et al. 1997), and they flow collectively parallel to the layers with a Lorentz force, which causes flow voltage and hence the flow resistance obtained. The mid point of the center of the plateaus in the flow-resistance obtained from both direction of scanning angle has been taken as a tentatively aligned position to the superconducting layers with a resolution of 0.005° . Refinement of the aligned

position to the field has been made to show the maximum flow-resistance. Details of the JV flow measurements are also described in Ref. (Ooi et al. 2002). Figure 3 (c) shows a typical curve of the flow resistance at 70 K. The flow resistance begins to oscillate periodically from below 10 kOe, reaches to its maximum at 20 kOe, and suddenly drops to zero at around 23 kOe. This drop is caused by the misalignment of the sample. When the magnetic component H_c along the c-axis of the applied field H reaches to H_{c1} , then, PVs penetrate to the sample, are pinned at pinning centers (crystal defects), cause JVs pinning with cooperative phenomena, and reduce the JV flow-resistance. Refinement of the aligned position to the field has been made to show the maximum of the flow-resistance as large as possible in magnetic field. Then, the resistance reaches to saturate with a finite value after the maximum with increasing the parallel field. This angle is set as an optimum value for evaluating a magnetic phase of JVs.

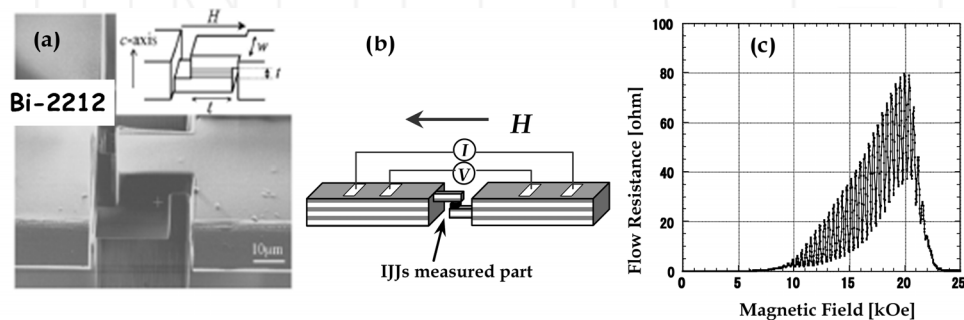


Fig. 3. (a) Secondary ion image of the measured sample after the FIB fabrication. Inset in (a) shows a schematic drawing of the sample geometry and applied magnetic field. (b) Schematic drawing of IJJs parts and electrodes configuration for the transport measurements. (c) Typical example of Josephson vortex flow-resistance against magnetic field.

In section 5, for the application of the periodic oscillations to measure a magnetic field precisely, pair of modulation coils has been set to the both side of the sample in Fig.3 (b) in addition to the main superconducting 8 Tesla split magnet. It produces about 200 Oe.

3. Flow resistance of Josephson vortices

When vortices in superconductors are driven by the applied current perpendicular to the direction of magnetic field, the vortices flow by the Lorentz force in the direction perpendicular to the field and the current. Movement of the vortex core, which is in normal state, causes a dissipation and hence flow-resistance. The flow velocity is determined by the vortex states and also the superconducting media. Vortex states are related to the glass state, vortex-lattice state, for example. Superconductors have many kinds of imperfections; inhomogeneity of the materials, defects (stacking fault, dislocations, etc), and impurities. These imperfections sometimes become pinning centers for vortices and the vortex states cause a flow-resistance (Tinkham 1975; Blatter 1994). In HTSCs, PVs flow as to the vortex motion of vortices in conventional superconductors, although they have a variety of vortex phases. As HTSCs have a high T_c , the vortices are easily influenced by the thermal fluctuation. Furthermore, PVs are weakly connected

between the superconducting layers through the insulating layer, which causes a complicated dissipation. On the other hand, the motion of JVs in HTSCs is quite different from that of PVs. JVs are located at the insulating layer as shown in Fig.2. They can easily move along the superconducting layers, but not along the perpendicular direction to the layers. This is so-called intrinsic pinning of JVs. For the applications of HTSCs to superconducting magnets, the intrinsic pinning mechanism is used to generate a magnetic field along the insulating layers.

3.1 Flow of Josephson vortices in HTSCs

Flow of JVs has been studied in artificially-made Josephson junctions. In principle, JV flows very fast close to the light velocity because of a very low dissipation without normal state core (Fujimaki 1987; Bulaevskii 1991). However, there are many imperfections in real materials, which lead to the larger dissipation and reduce the velocity. In HTSCs, Josephson junctions are formed intrinsically, consisted of a stack of atomic scale layers as shown in Fig.1 (b). In strongly anisotropic superconductors such as HTSCs, JV core is defined as Josephson length γs , where γ is the anisotropic parameter defined as λ_c/λ_{ab} (London penetration depth (λ_{ab} and λ_c)) and s is the interlayer spacing of superconducting layers, as shown in Fig.2 (a). JV flow accompanies a movement of JV core, which causes a dissipation of the *in-plane* resistivity ρ_{ab} and the *c-axis* quasi-particle tunneling resistivity ρ_c . Before discussing the flow resistivity ρ_{Jf} of JVs, we define the crossover magnetic field as $B_{cr} = \Phi_0/\pi\gamma s^2$, following to the definition of Koshelev 2000, where JVs start to overlap and dense distribution of JVs form JV lattice as shown in Fig.2 (c). B_{cr} in Bi-2212 ($\gamma = 500$) is about 6 kOe with $s = 1.5$ nm. This value is relatively small compared to YBCO, which has a small value of γ about 10 and has a crossover magnetic field larger than a few Tesla.

JV flow-resistivity ρ_{Jf} is expressed as $\rho_{Jf} \sim \pi\gamma s^2 B / (\Phi_0(\sigma_c + 0.27\sigma_{ab}/\gamma^2))$ for the magnetic field $B < B_{cr}$ (Koshelev 2000), where σ_c and σ_{ab} are the *c-axis* quasi-particle tunneling conductivity and the *in-plane* conductivity, respectively. In this magnetic field range, ρ_{Jf} shows linear dependence to B and is proportional to the number of JVs. In the magnetic fields of $B > B_{cr}$, $\rho_{Jf} \sim \rho_c B^2 / (B^2 + B_\sigma^2)$, where $B_\sigma^2 = \sigma_{ab}\Phi_0^2/2\pi^2\sigma_c\gamma^4 s^4$ and ρ_c is the *c-axis* resistivity. With increasing magnetic fields, flow resistivity gradually deviates from linear dependency, and saturates to ρ_c at the field B_σ for strong *in-plane* dissipation. There are two kinds of dissipation dominated; the *c-axis* dissipation channel ($\sigma_{ab}/\sigma_c \ll \gamma^2$) and *in-plane* dissipation channel ($\sigma_{ab}/\sigma_c \gg \gamma^2$). B_σ is much larger than B_{cr} . In Bi-2212, B_σ is about 40 kOe for $\gamma = 500$, $\sigma_{ab} = 50000 \Omega^{-1}\text{cm}^{-1}$, and $\sigma_c = 0.002 \Omega^{-1}\text{cm}^{-1}$.

Figure 4 shows a magnetic field dependence of JV flow-resistance of Bi-2212 measured at 70 K with dc current density of 60 A/cm². Bi-2212 belongs to the resume of $\sigma_{ab}/\sigma_c \ll \gamma^2$, estimated from the values in the last paragraph. Actually, the flow resistance increases linearly with magnetic field at lower magnetic fields, and shows an upward curvature at larger magnetic fields, which is the behaviour of the *in-plane* channel dominated flow resistivity (Koshelev 2000). At near the zero magnetic fields, the flow-resistance shows a downward curvature, which is considered as pinning effects of surface boundary of the junctions and pinning centres intrinsically existed in the sample.

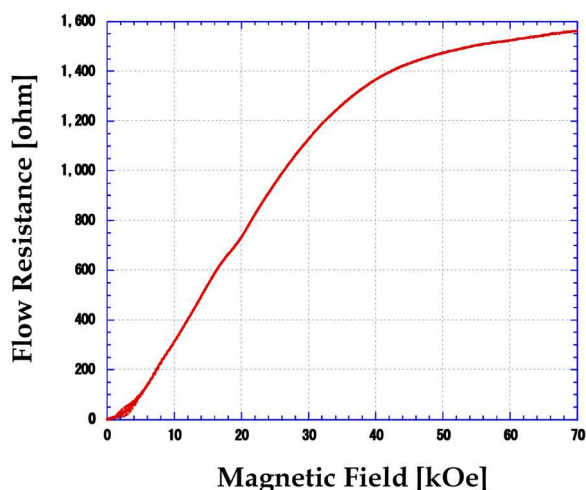


Fig. 4. Magnetic field dependence of the JV flow-resistance in Bi-2212 measured at 70K with dc current density of 60 A/cm². At lower magnetic fields, the flow-resistance shows linear magnetic field dependence, and saturates to a finite value at higher fields, which suggests the *in-plane* channel dominates in Bi-2212.

3.2 Periodic oscillations in flow resistance of Josephson vortices

In Fig.4, the JV flow-resistance of Bi-2212 was measured with dc current of 0.15 mA and the junction size of width 17.6 μm , length 14.0 μm , and thickness 1 μm . From the size of the sample, this current corresponds to the current density of about 60 A/cm². Figure 5 (a) shows current density dependence of the flow resistance of the sample at 70 K with the angle from the superconducting layers of 0.010 degree. Decreasing the current density from 60 A/cm², it can be clearly observed that the flow-resistance starts to oscillate at lower magnetic fields around 6-7 kOe below around 8 A/cm² (0.020 mA), and the oscillations disappear at higher magnetic fields. At lower current density than 8 A/cm², the oscillations become pronounced and the flow-resistance shows a maximum at around 40 kOe. The flow-resistance decreases from about 40 kOe, but still remains even at 70 kOe, which is the maximum magnetic field applied by the split superconducting magnet.

It is noted that the oscillations are observed only in sufficiently small current region. Figure 5 (b) shows an *I-V* characteristic of the junction size of width 18.0 μm , length 16.5 μm , and thickness 1 μm at 65K. *I-V* curves are plotted in magnetic fields from 14 kOe to 16 kOe for every 20 Oe. Each curve is shifted by a 1 mV step. At the magnetic fields where the flow-resistance shows minimum, the nonlinearity of *I-V* curves becomes large and a kink structure is seen at around 30-50 μA . The periodic nonlinearity corresponds to the periodic oscillation of the JV flow-resistance. In the current larger than 100 μA , the nonlinearity disappears. The current 30 μA corresponds to the current density of 9 A/cm². Appearance of the periodic oscillations at 30 μA (9 A/cm²) is quite well to coincide with the value of 8 A/cm² in the last paragraph.

Figure 6 (a) shows a part of Fig.3. (c), plotted from 15 to 18 kOe. The oscillations show quite constant periodicity H_p even in this magnetic field. The periodic oscillations are reproducibly observed in a wide temperature range from (T_c-3) to 4.2 K, and in a wide magnetic field range from B_{cr} to close to B_{c2} , which will be discussed in determining magnetic phases of JVs. We have investigated the origin of the periodicity by measuring the flow resistance on several samples with different width w . The width w is defined as the sample size in the perpendicular direction to the magnetic field shown in the inset of Fig.3(a).

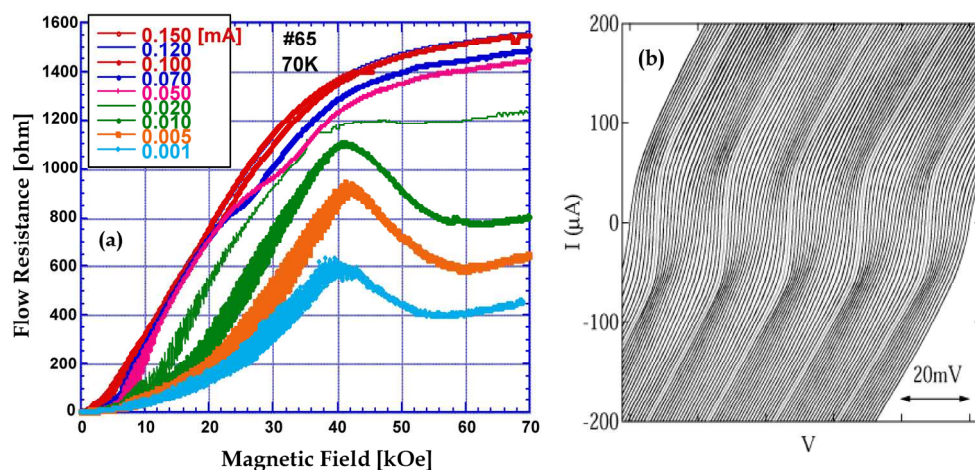


Fig. 5. (a) Current-dependency of the flow-resistance in a small current range. (b) I - V characteristic in magnetic fields from 14 kOe to 16 kOe for every 20 Oe at 65K. Each curve is shifted by a 1 mV step.

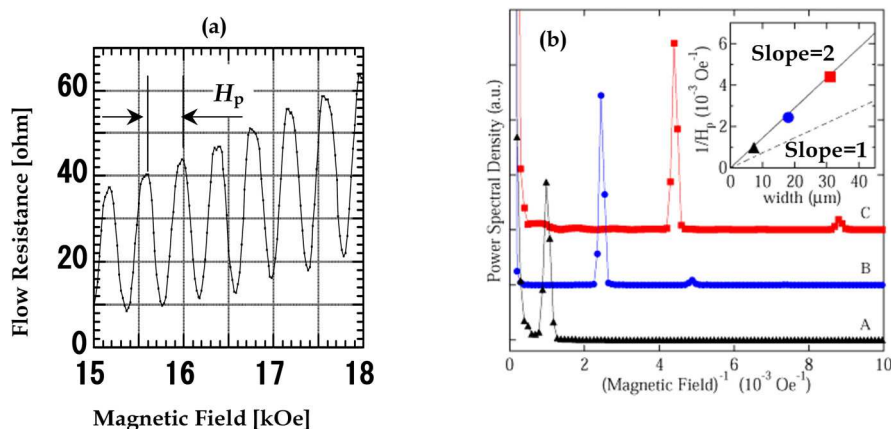


Fig. 6. (a) Periodic oscillations in JV flow-resistance; enlarged part of Fig.3. (b). (b) Power spectrum of the periodic oscillations in fast Fourier transform on samples A, B and C. Inset shows width (w) dependency of the inverse of H_p . The broken and solid lines represent $1/H_0(w)$ and its double, respectively.

Figure 6 (b) shows the fast Fourier transform of the periodic oscillations on samples A ($w=7.3 \mu\text{m}$), B ($w=18.0 \mu\text{m}$) and C ($w=31.0 \mu\text{m}$). The sharp fundamental peaks can be seen, which suggests that the periodicity H_p is quite constant in a wide range of fields and over the samples. The small peaks correspond to the second harmonic waves, which are caused by a little distortion from the sinusoidal curves. In the inset of Fig.6 (b), the position of the peaks is plotted against sample width (w). All the samples show a linear dependence to width (w) with a slope of 2, but not 1.

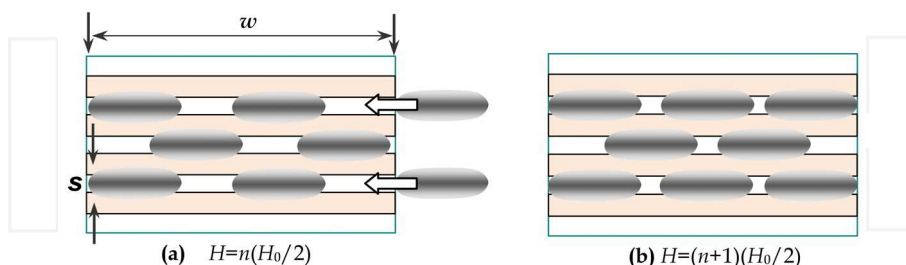


Fig. 7. Schematic drawing of Josephson vortex configuration to explain the magnetic period of the flow-resistance. The period indicates the magnetic increment of $\phi_0/2ws$, which means that the Josephson vortices form a triangular lattice above B_{cr} .

The value of the slope is very indicative for the interpretation of the periodic oscillations. When the JVs are supposed to be uniformly distributed in the junctions above B_{cr} , with increasing magnetic fields, JVs penetrate into each junction. Then, the increment of magnetic field ($H_0(w)$) to put one JV per one layer is ϕ_0/ws . Then, the slope $1/(\phi_0/ws)$ would be 1. However, the experiments show the value of 2. So, the slope is double of $1/(\phi_0/ws)$, and is rewritten as $2/(\phi_0/ws) = 1/(\phi_0/2ws)$. This means that, in a increment of magnetic field H_p , one JV penetrates into every two-junctions.

The above experimental results can be explained by assuming that the lattice structure of JV system is triangular, and, at both sides of the sample, a surface barrier, Bean-Livingston barrier, for example, acts on the JVs' lattice. Figure 7 shows schematic drawings of the JV penetration into the junctions as (a) $H_p = n(H_0(w)/2)$ and (b) $H_p = (n+1)(H_0(w)/2)$, where n is the number of JV at certain magnetic field. Figures 7 (a) and (b) show the examples of JV system, in which the JVs are distributed in the ordered states, matched exactly with the size of the sample. In Fig.7. (a) of flowing JV-lattice system, JVs enter from the right side and exit from the left side simultaneously. Then, the total potential in the JV-lattice becomes maximum. The average velocity of JV flow and hence the flow-resistance becomes minimum. With increasing the magnetic field from this situation, additional JVs are forced to enter into the ordered lattice by the applied current. The JV-lattice can then move more easily because the total potential decreases due to the mismatching between JV-lattice and the width of the sample. The flow resistance becomes larger than that of the matching situation. When the magnetic field exceeds $(n+1/2)(H_0(w)/2)$, the JV-lattice starts to form the next matching state as shown in Fig.7 (b). Therefore, it is plausible to consider that the oscillation period of the flow-resistance becomes half of $H_0(w)$. The effect of the boundary to the JV-lattice is crucial as shown in Fig.8. Difference in the two main effective width $\Delta w = |2l \sin \theta|$ shown in the inset of Fig.8 (b) acts to determine the beating period as a surface

barrier to the flowing JV-lattice. The period H_p is determined only by the effective width, which means that JV-lattice flows is strongly affected by the boundary (Ooi et al. 2004).

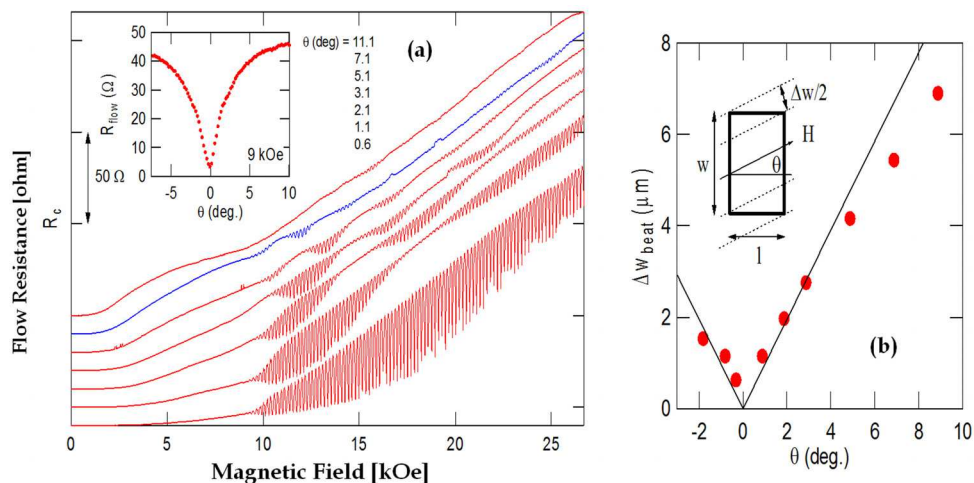


Fig. 8. (a) Beating in JV flow-resistance. The flow resistance was measured with changing the *in-plane* angle θ . With increasing angle θ , the beating effect becomes significant. Inset shows the angle dependence of the flow resistance at 9 kOe. (b) Difference of two effective widths as a function of θ estimated from the periods of beatings. Solid curve shows $\Delta w = |2l \sin \theta|$. A schematic drawing of the sample in an in-plane field is put in the inset to explain the effective width and definition of Δw .

The above mentioned interpretation can be applied to the I - V characteristics and the current density dependence of the oscillations in the magnetic fields qualitatively. When the surface potential is smaller than the energy of JV-system flowing with Lorentz force by the larger applied current, it is expected that the periodic oscillations would be smeared out. This is the speculation from the experimental results, but it was confirmed theoretically by analytical method (Koshelev 2002; Ikeda 2002) and numerical calculations (Machida 2003).

As the periodic oscillations can be observed in a lower current density, it is considered that as a ground state the JV-system is in a triangular lattice at intermediate magnetic fields. We also have investigated the JV flow-resistance with changing the anisotropy γ to confirm the effect of the anisotropy on forming a triangular lattice (Yu S. 2004 & 2007). As this is related to the magnetic phase diagram of Bi-2212 described in the next section, we only mentioned here that the starting magnetic field H_s of the periodic oscillations is inversely proportional to γ . This is also one evidence to prove the theories and the formation of triangular lattice. Furthermore, the triangular lattice of JV system changes to the rectangular lattice with changing the sample size smaller and increasing the magnetuc fields (Yu S. 2004 & Hirata K. 2003). The boundary magnetic field B_{TR} between triangular and rectangular lattice is defined as $B_{TR} = w\Phi_0 / 2\pi\gamma^2 s^3$ (Koshelev 2002), which is also well coincided with experiments (Yu S. 2004 & Hirata K. 2003). On contrary, it is useful to determine the anisotropic parameter from the JV flow resistance measurement directly. The periodic oscillations have a universal

nature of JV-system in a strongly anisotropic superconductors, and hence can be applied to determine the magnetic phases of JV-system and the magnetic field precisely, which will be discussed in section 4 and 5, respectively.

4. Magnetic phases of Josephson vortices

Magnetic phases of HTSCs have been well studied in the weakly anisotropic superconductors such as YBCO (Blatter et al. 1994). The first-order melting transition is one of the pronounced characters in HTSCs. In strongly anisotropic superconductors such as Bi-2212, theoretical approaches have been made extensively, but few experimental studies have been made due to the little change in free energy to confirm the phase boundary, as mentioned in the Introduction. One of the useful methods is to measure a flow resistance of JVs. This method is useful even in the vortex solid phase. In the solid phase, it is difficult to study the state because of that resistivity usually goes to zero due to the pinning effects from quenched disorder. However, a collective JV flow appears in the *c*-axis resistance even at low temperatures (Lee et al. 1995). The periodic oscillations mentioned above is an indirect experimental evidence of forming a triangular lattice in JV system of strongly anisotropic superconductors, but is considered to be a unique experimental probe to confirm the 3D-ordered state in JVs. Therefore we applied this method to determine magnetic phases in Bi-2212.

4.1 JV flow resistance at lower magnetic fields

To determine magnetic phases in Bi-2212, we apply the JV flow resistance method. The magnetic field region, in which we can observe the periodic oscillations, is assigned to the 3D-ordered state of JV system. In the measurements, the effect of the PVs is crucial, which are easily excited thermally in HTSCs with a strong anisotropy. As PVs are also incorporated with the misalignment of the parallel fields to the superconducting layers. However, the effect is much enhanced at higher magnetic fields, and there is no need to consider about the existence of PVs at lower fields. Figure 9 shows a JV flow resistance of the sample (width = 17 μm , length = 14 μm and thickness = 1 μm) as a function of the lower parallel field at the temperature close to T_c (85K) with an ac current of 1.0 μA . The periodic oscillations start at around 80.5 K, and are clearly seen from 80.0 K at 5.8 kOe, which is denoted as an oscillation-starting magnetic field of H_s . This magnetic field H_s corresponds to the boundary between a liquid state and a triangular lattice state. H_s has little temperature dependence seen from Fig.9. The boundary is almost independent of temperature. It is noted here that, at the temperatures without the oscillations in the flow resistance, the flow resistance increases proportional to the field and we can see a development of a hump shown as H_h in Fig.9. Just before the appearance of the oscillations, the hump H_h seems to jump to the starting field H_s of the oscillations with decreasing temperature. H_h also appears continuously as a kink in the flow resistance at about 3 kOe independent of temperature at lower temperatures (not shown here). This value of H_h is almost half of the starting field H_s , and is considered to relate to the formation of the JV lattice with a half filling to the layers (Ikeda 2002). As the half filling state is one of ordered state (Ikeda 2002), the increment of the flow resistance will be stopped as indicated in the experiments, considering from the matching effect of the JV half filling lattice to the sample width.

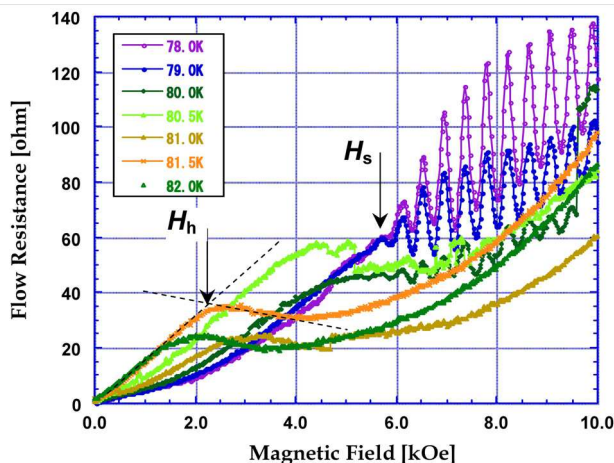


Fig. 9. Josephson-vortex flow resistance as a function of the parallel fields at the temperature close to T_c . We can find a hump, continuously connected to the beginning of the oscillations at 5.8 kOe with decreasing temperature.

4.2 JV flow resistance at higher magnetic fields

Figures 10 (a) and (b) show the flow resistance as a function of the parallel field at temperatures from 4.2 K to 80 K on the same sample in Fig.9. Below 20 K, we can observe a constant period H_p ($H_p = \phi_0 / (2ws)$) of the oscillations till 70 kOe. The flow resistance still increases in this temperature range. At intermediate temperatures from 30 K to 50 K, it shows a maximum and decreases and becomes constant at higher magnetic fields. But at higher temperatures it increases again. The decrease in flow resistance at the intermediate temperatures is not caused by the misalignment of the sample as following. In the case of the misalignment about 0.03° , on which the results are shown in Fig.3 (c), the resistance shows a maximum around 20 kOe and a sharp drop to zero at about 23 kOe. Incorporation of the PVs with the c -axis component of the field, JVs are easily pinned to the pinning sites, because of the strong pinning of the PVs at lower temperatures in Bi-2212 and of considering the free energy of the pinned JVs to the PVs (Koshelev 1999). Decrease of the flow resistance after the maximum may be caused by a disordered state of JVs magnetically and thermally from the 3D-ordered state. Above 60 K, the pinning strength of the PVs in Bi-2212 is decreased, which can explain the increment of the flow resistance. Then, it is considered that, when the sample is close to the aligned configuration like this experiment, the finite flow resistance in the intermediate temperatures at higher magnetic fields is an intrinsic one in JV system. With increasing temperature and magnetic field, it is suggested that JV system changes from a triangular-lattice state to another one. The phase boundaries are drawn in Fig. 11 as a magnetic phase diagram of JV system. This may be considered as a magnetically induced transition at a constant temperature, and as a thermally induced transition at a constant field. In this state, JV system is not in an ordered state in 3D, along the c -axis or along the a - or b -axis also. This state may be in a 2D quasi-long-range ordered state suggested in Ref. (Hu & Tachiki 2000). Further experiments should be made to make clear the phase diagram of JVs.

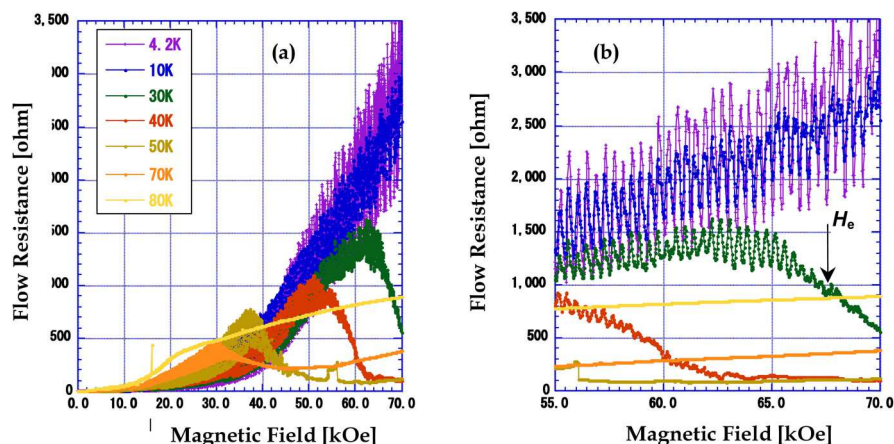


Fig. 10. Josephson-vortex flow resistance as a function of the parallel fields at various temperatures (a) and the enlarged part of (b) at higher magnetic fields (b). H_e denotes the end of the periodic oscillations.

The flow resistance increases monotonously with the periodic oscillations at lower temperatures with increasing magnetic field. With increasing temperature, the flow resistance always shows a maximum and decreases to a finite value in the flow resistance, in which the oscillations stop just before reaching to the finite flow resistance. To define the characteristic magnetic field H_e , a criterion was taken at some magnitude of the resistivity in the amplitude of the oscillations. Reproducibility was confirmed several times with changing the angle between the superconducting layers and the magnetic field, which showed a few kOe as in experimental error. Therefore, this characteristic feature of the flow resistance at higher temperature is considered as an intrinsic behaviour in JV flow.

In Fig.11, the phase boundaries obtained from the flow resistance measurements are shown. The magnetic field H_e in Fig.10 (b), indicated by the arrow, corresponds to the upper boundary of the 3D-ordered phase, which is defined as the magnetic field for the oscillations to be stopped. The boundary H_e decreases steeply at the temperatures lower than 40 K, is saturated at about 50kOe, and suddenly decreases at about 75 K towards 0 kOe at T_c . This means that the oscillations continue even in higher magnetic fields than 70kOe below 40 K, and JV system is in the 3D-ordered state below H_e and above H_s boundaries. It is noted here that H_s is almost constant with temperature because of depending only on the anisotropy γ and the samples width w .

Considering about the JV state in this magnetic field and temperature region, it is suggested that the JV state may really change from the 3D-ordered state to the other. In the flow resistance above H_e , the resistance always decreases to a finite value after the periodic oscillations in the region B of Fig.11, which may suggest that the JV state is in disordered along the c -axis, as the *in-plane* disorder causes an enhancement of the flow resistance with less effective potential barrier to the dynamical movement of JVs. With changing the angle between the layers and the magnetic field, little effect and the less systematic changes to the flow resistance were observed concerning on the decrement of the resistance. Then, we can

get rid of the effect of the PVs caused by the misalignment in the higher magnetic fields. Then, the decrease of the resistance in this region may be caused by the excitation of abundant amount of pancake-vortex/anti-vortex pairs, thermally and magnetically, because the pinning force of the PVs is very weak in this magnetic field and temperature range far above the irreversibility region of the PVs.

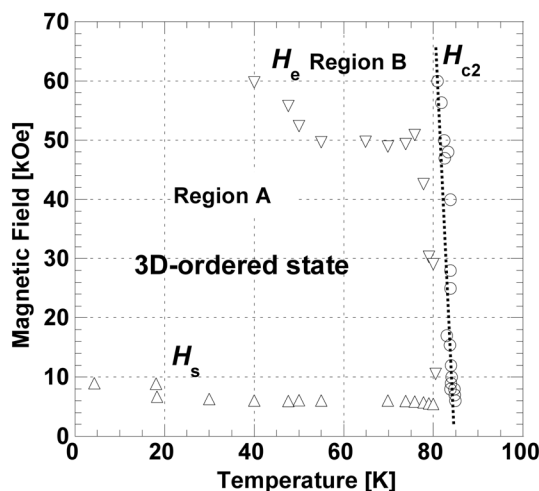


Fig. 11. Magnetic phase diagram of Josephson vortices in Bi-2212, obtained from the flow-resistance measurements. Open and solid symbols correspond to the boundaries defined on the sample in Fig. 10 and another sample with smaller γ , respectively.

To study the JV state above/below the upper boundary H_e , shown in Fig.11 as the region A/B, respectively, I - V measurements have been made. In Fig.12, the power-law dependence to the magnetic field in sample A is shown as the exponent $\alpha(T,H)$ of $V=AI^\alpha$, obtained from the I - V characteristics. In the figure, the data are plotted every 10 kOe, and are shifted in both sides at every magnetic field to see clearly. The measurements were made in the current range well below the critical current density of Bi-2212, in which the periodic oscillations can be observed in the region A. It shows a distinct change in $\alpha(T,H)$ to 1.6 and 2.0 above 50 kOe, compared with those at lower magnetic fields. The change in α is well coincided with the magnetic phase diagram shown in Fig.11.

Hu and Tachiki (Hu & Tachiki 2000) have studied on JV system, the first-order melting transition, phase transition between 3D ordered state and 2D QLRO (quasi-long-range ordered) state, and also the power-law dependence in K-T phase with Monte Carlo simulations. The region B in Fig.11 obtained from the present measurements is considered to correspond to the K-T phase in Fig.10 of Ref. (Hu & Tachiki 2000). Temperature dependence of $\alpha(T,H)$ is not explicitly shown in Eq.18; $\alpha=1+Y\pi/(k_B T)$ of Ref. (Hu & Tachiki 2004). However, the behavior of the exponent $\alpha(T,H)$ is inferred from the temperature dependence of the calculated helicity modulus Y with $\gamma=8$ and 20 in Fig.10 of Ref. (Hu & Tachiki 2000), which decreases with increasing temperature. Assuming that the behavior of Y in temperature is the same as that in a larger anisotropic value of Bi-2212, $\alpha(T,H)$ decreases with

increasing temperature. This shows a little different behavior from the experimental results. Furthermore, there have not been observed the oscillatory behavior of the melting transition and the first-order phase transition in the experiments on Bi-2212. It may need much more sensitive measurements than the present experimental set-up. Further experiments will be needed to make this JV state clear.

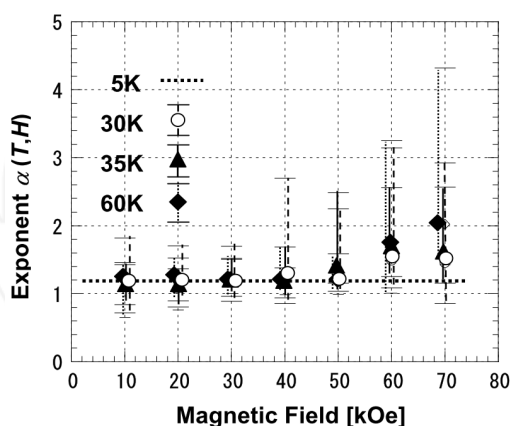


Fig. 12. Magnetic field dependence of the exponent $\alpha(T, H)$ in the I - V characteristics at 5, 30, 35, 60 K with $V=AI^\alpha$.

We have tried to confirm the effect of the anisotropy γ in the boundary with changing the anisotropy (Yu et al. 2005 & 2007). The tendency of the change of H_c is a good indication to increase the doping level of carriers into Bi-2212, namely, decreasing the anisotropic parameter γ , which can be related to the weaker anisotropic superconductors such as YBCO continuously.

5. Application of periodic oscillations for magnetic sensor

With magnetic-field cycles, the flow resistance reproduces quite well in a wide range of temperature, in which the oscillations can be observed. However, with heating/cooling cycles at a constant magnetic field, the flow resistance shows an irreversible feature as shown in Fig.13. After applying the magnetic field up to 20 kOe at 5 K with a zero-field cooling and confirming the periodic oscillations, for example, with increasing temperature, the flow resistance suddenly drops close to zero at about 50 K, even if a finite flow resistance can be observed at the same temperature and magnetic field with the zero-field cooling and magnetic-field cycles. This can be seen at every magnetic field where the oscillations can be observed. This may be closely related to the JV states, which have never been made clear before on the strongly anisotropic HTSCs experimentally. It has been theoretically discussed just after the discovery of HTSCs (Chakravaty et al. 1990; Blatter et al. 1994), and recently with Monte-Carlo simulations (Hu & Tachiki 2004). In the JV system, it is predicted that pairs of pancake vortex-anti-vortex are easily excited thermally. If these pancake pairs are excited in the JV system, they are easily pinned at the intrinsic pinning centers of Bi-2212, because this region belongs to the irreversible one in the magnetic phase diagram of Bi-2212 with the perpendicular field.

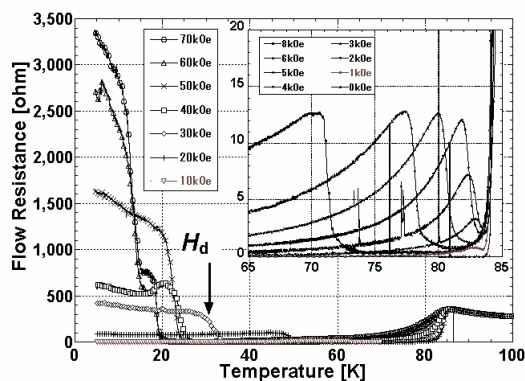


Fig. 13. Temperature dependence of the flow resistance at a constant magnetic field measured in a zero-field cooling&warming-up process. Inset shows the flow resistance at lower magnetic field region.

However, the magnetic field, at which the flow resistance suddenly drops, cannot be seen in the temperature dependence of magnetic-field cycles at every temperature. There exists only a boundary between the regions on the periodic oscillations and of the finite flow resistance without the oscillations at high temperatures and magnetic fields (Hirata et al. 2004). This boundary may correspond to the continuously melting transition (Hu & Tachiki 2004). In the field-cooling process, it is considered that these PV pairs are excited thermally at higher temperatures than the irreversibility temperature, they are frozen to the pinning centers with decreasing temperature, and the flow resistance does not show any sharp increment at low temperatures. Although there are still incomprehensive problems in the JV system, for the application, we have to avoid a temperature increase of the sensor higher than 50 K at 20 kOe, for example, as shown in Fig.13.

Using a pair of small coils, we have measured the JV flow resistance. Figure 14 shows the results of the JV flow resistance measured at the main magnetic field H_m with an interval of 20 Oe, an ac current of 1.0 μA , and the size of the junction $t = 1.5 \mu\text{m}$, $w = 11.2 \mu\text{m}$, $l = 12.4 \mu\text{m}$ at 70.0 K as an example. The period H_p is obtained as about 900 Oe independent of temperature and magnetic field, which is well coincided with the calculated value H_p as 924 Oe, considering about Josephson penetration length and the damaged width by the FIB-fabrication of the sample (Hirata et al. 2004). Fixing the field H_m at 15.2 kOe, a modulation field H_i was applied to measure a resistance change by the JV flow. The signal was directly obtained from LR-700 as a raw output voltage without any filters, which is shown in Fig.14. To compare the magnitude of the flow resistance at 15.2 kOe of 70.0 K in Fig.13 with that in Fig.14, it is just a bit smaller than that about 30 ohm. Carrying out the measurements of the flow resistance, we have recognized that the c -axis resistance becomes very sensitive in superconducting state. By the extra set-up of the coils to the normal measurements, it may cause some noise in the circuit of LR-700.

In Fig.14, it is apparently seen that the signal is well scattered. This means that the JV flow velocity changes within less than 0.1 sec, because the measurements were made with the ac current of 13.6 Hz. This has been discussed by Machida (Machida 2003). The JV flow is a

dynamical effect, interacting to each other. And JVs go over the potential barriers at the both edges of the sample, which is one of the principal reasons for the periodic oscillations, while inside the sample edges JVs move almost freely accompanied with some dissipation by the quasi-particles (Koshelev 2000). When we take a snapshot to see the behavior of the JV flow, there might be some distribution in velocity of JV-lattice flow. The velocity is determined mainly by the matching effect of JV lattice to the width of the sample (Machida 2003). Making these noise characteristics clear, it may be effective to take a noise spectrum of the flow voltage, which will be developed and obtained near future.

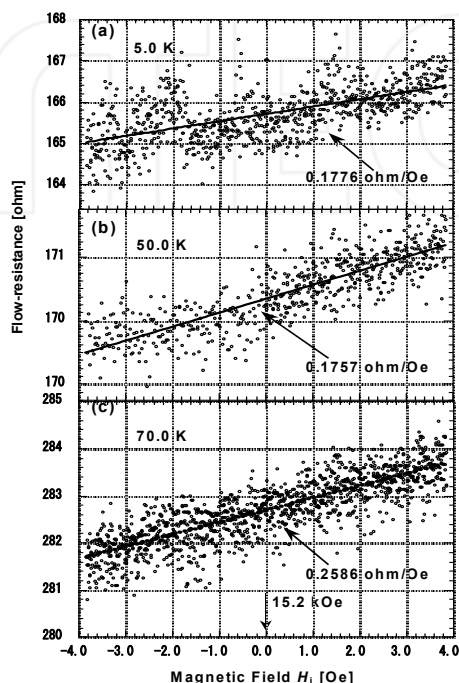


Fig. 14. Flow-resistance (a), (b) and (c) at the main fields $H_m=15.2$ kOe as a function of a modulation field H_i of small coils at 5, 50 and 70 K, respectively. The solid lines show a fitting line to the data, and show a good linearity with a slope of 0.1776, 0.1757 and 0.2586 ohm/Oe, respectively.

It is worth for being noted that the linearity of the flow resistance to H_i is relatively good, which is shown as solid lines in Fig.14. The solid lines were obtained with a square-root minimum fitting method. The slope of the line is calculated as 0.2568 ohm/Oe at 70 K shown in Fig.14 (c), for example. The fitting line is considered to indicate average values in time at each field. And the measurement is easily improved to make averaging the voltage in the interval of a few second or longer. When we need to measure a high magnetic field precisely, we are usually using the magnetic field in a steady state; apparatus of nuclear magnetic resonance and magnetic resonance imaging, for example. It is also benefit for this magnetic-field sensor to put into the low T_c superconducting magnets, as they are using at a liquid He temperature, and the temperature is very stable. Once if we make a calibration of

the sensors at 4.2 K and a fixed magnetic field, we can get a precise control of the magnetic field within a μT range.

6. Conclusion

In conclusion, we have measured JV flow-resistance on the in-line symmetric IJJs of Bi-2212 single crystals to study on the flow mechanism of JVs and on the dynamics of moving JVs. A pronounced feature has been found in the flow resistance. Periodic oscillations have been observed with sweeping the magnetic field parallel to the layers. The oscillations have been found in the wide range of the parallel fields larger than 6kOe and only in the smaller current region than about 10 A/cm². The period of the oscillations is inversely proportional to the width of the samples, and it corresponds to adding "one" flux quantum per "two" IJJs. These results suggest that the JVs form a triangular lattice as a ground state, which is related to the commensurability between the sample width and the lattice spacing of JVs along the layers in the present experiments using small IJJs.

We have studied the JV states with measuring the flow resistance. From the measurements, we can determine the 3D-ordered phase of JVs, in which JVs are well ordered. This has been never determined with other methods in strongly anisotropic superconductors. Furthermore, by the measurements of temperature dependence of the flow resistance, we find a sudden drop in the resistance in the zero-field cooling&warming-up process. The sudden drop is explained by the thermal and magnetical excitation of pancake vortex/anti-vortex pairs, which is an intrinsic property of Bi-2212. The boundary of the excitation exists between 20-30K above 15kOe and above 30K at lower magnetic fields. This boundary limits the application of HTSC materials in the magnetic fields.

We also have characterized the JV flow device as a magnetic sensor to measure the flow-resistance in Bi-2212 IJJs, using a remarkable feature of the periodic oscillations. The device has an irreversible character in temperature-cycles at high magnetic fields, which is caused by the thermal excitation of pancake vortex-anti-vortex pairs. Using a pair of small coils under high magnetic fields, good linearity of the flow-resistance was obtained to the internal field H_i . There is also a problem with noise, which may be caused by the intrinsic behavior of JV flow. However, it can be improved easily by the measurement method. The linearity of the flow-resistance to the small field H_i indicate that, once the device is calibrated, it has a high potential to measure and control high magnetic fields in Tesla range with a μT accuracy.

7. Acknowledgment

I acknowledged to Dr. S. Ooi for the fabrications of junctions and for useful discussions, and Dr. T. Mochiku for providing us single crystals of Bi-2212.

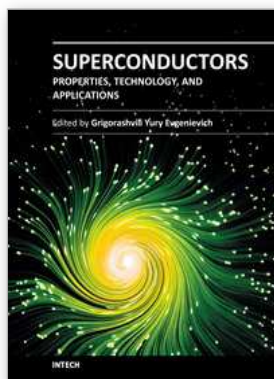
8. References

- Bean C.P. & Livingston J.D. (1964). Surface Barrier in Type-II Superconductors, *Phys. Rev. Letters* Vol.12, pp.14-16

- Balents L. & Nelson D.R. (1995). Quantum Smectic and Supersolid order in Helium Films and Vortex Arrays, *Phys. Rev. B* Vol. 52, pp.12951-12968
- Blatter G.; Ivlev B., & Ovchinnikov Y. (1990). Kosterlitz-Thouless transition in the smectic vortex state of a layered superconductor, *Phys. Rev. Letters* vol. 66, pp. 2392-2395
- Blatter G.; Ivlev B. & Rhyner J. (1991). Kosterlitz-Thouless Transition in the Smectic Vortex State of a Layered Superconductor, *Phys. Rev. Letters* Vol.66, pp.2392-2395
- Blatter G.; Feigel'man M.V., Geshkenbein V.B., Larkin A.I. & Vinokur V.M. (1994). Vortices in high-temperature superconductors, *Rev. Mod. Phys.* Vol.66, pp.1125-1388
- Bulaevskii L. & Clem J.R. (1991). Vortex lattice of highly anisotropic layered superconductors in strong, parallel magnetic fields, *Phys. Rev. B* Vol. 44, pp.10234-10238
- Chakravaty S.; Ivlev B. & Ovchinnikov Y. (1990), Resistivity of High-Temperature Superconductors: Is the Vortex State a Liquid?, *Phys. Rev. Letters* Vol.64, pp.3187-3190
- Fuhrer M. S.; Ino K., Oka K., Nishihara Y. & Zettl A. (1997). Observation of Josephson Vortex Lattice Melting in a Highly Anisotropic Superconductor, *Solid State Commun.* Vol.101, pp. 841-845
- Gordeev S.N.; Zhukov A.A., de Groot P.A.J., Jansen A.G.M., Gagnon R. & Taillefer L. (2000). Oscillatory Melting Temperature of the Vortex Smectic Phase in Layered Superconductors, *Phys. Rev. Letters* Vol.85 pp.4594-4597
- Hechtfisher G.; Kleiner R., Schlenga K., Walkenhorst W. & Muller P. (1997). Collective motion of Josephson vortices in intrinsic Josephson junctions in $\text{Bi}_2\text{Sr}_2\text{CaCu}_2\text{O}_{8+y}$, *Phys. Rev. B* Vol.55, pp.14638-14644
- Hess H.F.; Murray C.A. & Waszczak J.V. (1994). Flux Lattice and Vortex Structure in 2H-NbSe_2 in Inclined Fields, *Phys. Rev. B* Vol.50, pp.16528-16540
- Hirata K.; Ooi S., Sadki E.H. & Mochiku T. (2003). Josephson Vortex flow in $\text{Bi}_2\text{Sr}_2\text{CaCu}_2\text{O}_{8+y}$, *Physica B* Vol.329-333 pp.1332-1333
- Hirata K.; Ooi S., Yu S., Sadki E.H. & Mochiku T. (2004). Josephson Vortex States in $\text{Bi}_2\text{Sr}_2\text{CaCu}_2\text{O}_{8+\delta}$ Obtained from Vortex Flow Resistance measurements, *Physica C* Vol.412-414 pp.449-453
- Hirata K.; Ooi S., Yu S., Sadki E.H. & Mochiku T. (2004). Novel Magnetic Sensors using High T_c Superconductors, *Supercon. Sci. Technol.* Vol.17 pp.S432-S435
- Hu X. & Tachiki M. (2000). Possible Tricritical Point in Phase Diagrams of Interlayer Josephson-Vortex Systems in High- T_c Superconductors, *Phys. Rev. Letters* Vol.85 pp.2577-2580
- Hu X. & Tachiki M. (2004). Decoupled two-dimensional superconductivity and continuous melting transition in layered superconductors immersed in a parallel magnetic field, *Phys. Rev. B*, vol. 70, pp. 064506-1- 13
- Ikeda R.; (2002). Josephson Vortex State in Intermediate Fields, *J. Phys. Soc. Jpn.*, vol. 71, pp. 587-593

- Ishida T.; Okuda K., Ryukov A.I., Tajima S. & Terasaki I. (1998). In-Plane Anisotropy of Vortex-Lattice Melting in Large $\text{YBa}_2\text{Cu}_3\text{O}_7$ Single Crystals, *Phys. Rev. B* Vol.58, pp.5222-5225.
- Ivlev B.I.; Kopnin N.B. & Pokrovsky V.L. (1990). Shear Instabilities of a Vortex Lattice in Layered Superconductors, *J. Low Temp. Phys.* Vol.80, pp.187-195
- Kim S. -J.; Latyshev Y.I. & Yamashita T. (1999). Submicron stacked-junction fabrication from whiskers by focused-ion-beam etching, *Appl. Phys. Letters* Vol.74 pp.1156-1158
- Kleiner R.; Steinmeyer F., Kunkel G. & Muller P. (1992). Intrinsic Josephson Effects in $\text{Bi}_2\text{Sr}_2\text{CaCu}_2\text{O}_8$ Single Crystals, *Phys. Rev. Letters* Vol.68, pp.2394-2397
- Koshelev A.; (1999). Crossing Lattices, Vortex Chains, and Angular Dependence of Melting Line in Layered Superconductors, *Phys. Rev. Letters* Vol.83 pp.187-190
- Koshelev A.; (2000). Role of In-Plane Dissipation in Dynamics of a Josephson Vortex Lattice in High-Temperature Superconductors, *Phys. Rev. B*, vol. 62, pp. R3616-3619
- Koshelev A.; (2002). Edge Critical Current of Dense Josephson Vortex Lattice in Layered Superconductors, *Phys. Rev. B* Vol.66 pp.224514-1-6
- Kwok W.K.; Fendrich J., Welp U., Fleshler S., Downey J. & Crabtree G.W. (1994). Suppression of the First Order Vortex Melting Transition by Intrinsic Pinning in $\text{YBa}_2\text{Cu}_3\text{O}_{7-\delta}$, *Phys. Rev. Letters* Vol.72, pp.1088-1091
- Lee J.U.; Nordman J.E. & Hohenwarter G. (1995). Josephson Vortex Flow in Superconducting Single-Crystal $\text{Bi}_2\text{Sr}_2\text{CaCu}_2\text{O}_x$, *Appl. Phys. Lett.* vol. 67, pp. 1471-1473
- Machida M. (2003). Dynamical Matching of Josephson Vortex Lattice with Sample Edge in Layered High- T_c Superconductors: Origin of the Periodic Oscillations of Flow Resistance, *Phys. Rev. Letters* vol. 90, pp. 037001-1-4
- Mirkovic J.; Savel'ev S.E., Sugawara E. & Kadowaki K. (2001). Stepwise Behavior of Vortex-Lattice Melting Transition in Tilted Magnetic Fields in Single Crystals of $\text{Bi}_2\text{Sr}_2\text{CaCu}_2\text{O}_{8+\delta}$, *Phys. Rev. Letters* vol. 85, pp. 886-889
- Mochiku T.; Hirata K. & Kadowaki K. (1997). Crystallinity Improvement of $\text{Bi}_2\text{Sr}_2\text{CaCu}_2\text{O}_{8+\delta}$ Single Crystal by TSFZ Method, *Physica C* 282-287 (1997) 475-476.
- Fujimaki A.; Nakajima K. & Sawada Y. (1987). Spatiotemporal Observation of the Soliton-Antisoliton Collision in a Josephson Transmission Line, *Phys. Rev. Letters* vol. 59, pp. 2895-2899
- Ooi S.; Mochiku T. & Hirata K. (2002). Periodic Oscillations of Josephson-Vortex Flow Resistance in $\text{Bi}_2\text{Sr}_2\text{CaCu}_2\text{O}_{8+y}$, *Phys. Rev. Letters* Vol. 89 247002-1-4
- Ooi S.; Mochiku T., Yu S., Ishikawa H. & Hirata K. (2004). Beats of Josephson-Vortex Flow Oscillations, *Physica C* Vol.412-414 pp.454-457
- Schilling A.; Fischer R.A., Phillips N.E., Welp U., Kwok W.K. & Crabtree G.W. (1997). Anisotropic Latent Heat of Vortex-Lattice Melting in Untwinned $\text{YBa}_2\text{Cu}_3\text{O}_{7-\delta}$, *Phys. Rev. Letters* Vol.78, pp.4833-4836.
- Tinkham M.; (1975). *Introduction to Superconductivity*, McGraw-Hill, ISBN 0-07-064877-8, USA
- Rapp M.; Murk A., Semerad R. & Prusseit W. (1996). c-Axis Conductivity and Intrinsic Josephson Effects in $\text{YBa}_2\text{Cu}_3\text{O}_{7-\delta}$, *Phys. Rev. Letters* Vol.77, pp.928-931

- Zeldov E.; Majer D., Konczykowski M., Geshkenbein V.B., Vinokur V.M. & Shtrikman H. (1995). Thermodynamic Observation of First-Order Vortex-Lattice Melting Transition, *Nature* (London) Vol.375, pp.373-376
- Yethiraj M.; Mook H.A., Wignall G.D., Cubitt R., Forgan E.M., Paul D.M. & Armstrong T. (1993). Small-Angle Neutron Scattering Study of Flux Line Lattices in Twinned $\text{YBa}_2\text{Cu}_3\text{O}_{7-\delta}$, *Phys. Rev. Letters* Vol.70, pp.857-860
- Yu S.; Ooi S., Mochiku T. & Hirata K. (2005). Anisotropy Dependence of Josephson-Vortex flow Resistance, *Physica C* Vol.426-431 pp.51-55
- Yu S.; Ooi S., Mochiku T. & Hirata K. (2007). Anisotropy Dependence of Triangular lattice Formation of Josephson Vortices in $\text{Bi}_2\text{Sr}_2\text{CaCu}_2\text{O}_{8+y}$, *Phys. Rev. B* Vol. 76 pp. 092505-1-4



Superconductors - Properties, Technology, and Applications

Edited by Dr. Yury Grigorashvili

ISBN 978-953-51-0545-9

Hard cover, 436 pages

Publisher InTech

Published online 20, April, 2012

Published in print edition April, 2012

Book "Superconductors - Properties, Technology, and Applications" gives an overview of major problems encountered in this field of study. Most of the material presented in this book is the result of authors' own research that has been carried out over a long period of time. A number of chapters thoroughly describe the fundamental electrical and structural properties of the superconductors as well as the methods researching those properties. The sourcebook comprehensively covers the advanced techniques and concepts of superconductivity. It's intended for a wide range of readers.

How to reference

In order to correctly reference this scholarly work, feel free to copy and paste the following:

Kazuto Hirata (2012). Josephson Vortices in High Tc Superconductors, Superconductors - Properties, Technology, and Applications, Dr. Yury Grigorashvili (Ed.), ISBN: 978-953-51-0545-9, InTech, Available from: <http://www.intechopen.com/books/superconductors-properties-technology-and-applications/josephson-vortices-in-high-tc-superconductors>

INTeCH
open science | open minds

InTech Europe

University Campus STeP Ri
Slavka Krautzeka 83/A
51000 Rijeka, Croatia
Phone: +385 (51) 770 447
Fax: +385 (51) 686 166
www.intechopen.com

InTech China

Unit 405, Office Block, Hotel Equatorial Shanghai
No.65, Yan An Road (West), Shanghai, 200040, China
中国上海市延安西路65号上海国际贵都大饭店办公楼405单元
Phone: +86-21-62489820
Fax: +86-21-62489821